PCCP

Accepted Manuscript

ROYAL SOCIETY OF CHEMISTRY

www.rsc.org/pccp

Journal Name

ARTICLE

Reproducible, stable and fast electrochemical activity from easy to make graphene on copper electrodes

Received 00th January 20xx,
Accepted 00th January 20xx

DOI: 10.1039/x0xx00000x

www.rsc.org/

Concha Bosch-Navarro,[*,a,b] Zachary P. L. Laker,[a] Jonathan P. Rourke[b] and Neil R. Wilson,[a]

The electrochemical activity of graphene is of fundamental importance to applications from energy storage to sensing, but has proved difficult to unambiguously determine due to the challenges innate to fabricating well defined graphene electrodes free from contamination. Here, we report the electrochemical activity of chemical vapour deposition (CVD) graphene grown on copper foil without further treatment, through appropriate choice of electrolyte. Fast electron transfer kinetics are observed for both inner and outer sphere redox couples with fully covered graphene on copper electrodes (ko = 0.014 ± 0.0005 cm s^{-1} or ko = 0.012 ± 0.001 cm s^{-1} for potassium ferrocyanide (II) and hexaammineruthenium (III) chloride, respectively). Unlike highly oriented pyrolytic graphite electrodes, the electrochemical response of the graphene on copper electrodes is stable, with no apparent electrode fouling even with inner sphere redox couples, and reproducible independent of the time between growth and measurement. Comparison between fully covered electrodes, and partial coverage of graphene with varying graphene grain sizes (from roughly 50 µm to <10 µm) shows that in this instance the basal plane of graphene is electrochemically active. These CVD grown graphene on copper electrodes are quick, cheap and reproducible to make and hence provide a convenient platform for further investigation of graphene electrochemistry and the effect of covalent and non-covalent modification.

Introduction

Graphene has attracted extensive research interest due to its unique electronic, mechanical and optical properties.[1,2] Moreover, its 2D structure composed of only sp^2 carbon atoms in a honeycomb lattice results in a high surface area (2630 m^2 g^{-1}).[3] Thus, surface chemistry is of fundament importance for the properties and applications of such a novel material. Graphene's electrochemical activity is of particular interest,[4,5] with relevance for applications such as energy storage and generation and electrochemical sensing as well as for understanding graphene's role in enhancing or preventing corrosion. However, the electrochemical properties of graphene remain controversial, due in part to the effects of the processing typically required to fabricate graphene electrodes.

Graphene can be obtained following chemical or physical methodologies.[3,6] Although chemical methodologies (*e.g.* synthesis by reduction of graphene oxide[3,7–9] or liquid-phase exfoliation of graphite)[10] are more easily scalable, they usually lead to highly defective graphene. They are amenable to solution processing, which makes electrode fabrication simple but reduces the control over the deposition morphology and number of layers of graphene. Hence, from a fundamental electrochemistry point of view, physical methods for obtaining graphene are more interesting. Mechanical exfoliation of graphite[11] provides high quality graphene but forms only small isolated flakes (which must then be electrically connected) and possible contamination from the adhesive tape complicates interpretation of its electrochemical response. Chemical vapour deposition (CVD) is a promising route to the formation of large area, high quality graphene.[12] Graphene is formed by CVD through the decomposition of a carbon containing feedstock on a substrate at high temperature; the most common substrates are nickel and copper. On both, graphene can form a continuous layer across the whole substrate but the resultant film is polycrystalline, i.e. composed of grains of graphene of different orientations connected by grain boundaries. CVD growth on copper can be self-limiting and hence form predominantly monolayer graphene; significant amounts of research effort have been devoted to improving and understanding CVD growth of graphene on copper, resulting in increases in the grain size of graphene on copper films towards the millimetre scale. By contrast, CVD growth of graphene on nickel typically results in small (of order micrometre or less) grain sizes and many multi-layer regions. Hence CVD growth of graphene on copper is increasingly being used for electrical applications where it has been shown to have comparable properties to mechanically exfoliated graphene.[13]

Surprisingly, just a small fraction of the many electrochemical studies of graphene have used CVD graphene,[14–22] probably

[a] *Department of Physics, University of Warwick, Coventry, CV4 7AL, UK*
[b] *Department of Chemistry, University of Warwick, Coventry, CV4 7AL, UK.*
† Electronic Supplementary Information (ESI) available Additional information includes SEM, STM and TEM images, a schematic of the electrochemical set-up and additional electrochemical information.. See DOI: 10.1039/x0xx00000x

because of the difficulties that can be involved in subsequent electrode preparation. Although some electrochemical studies have directly used CVD graphene grown on nickel without further processing,[16] interpretation of these in terms of the electrochemical activity of graphene is limited by the unavoidable mixture of single- to few-layer graphene, large concentration of defects and electrochemical activity of the underlying nickel substrate. For CVD graphene on copper, electrochemical investigations have been hampered by the reactivity of the copper substrate, although this has enabled the use of electrochemistry to evaluate the surface coverage of graphene on copper.[19] To avoid substrate interference, graphene is instead usually transferred from the growth substrate to an insulating substrate.[20,21,23–25] However, transferring graphene is time consuming, requires etchants to remove the metal substrate and typically involves the use of polymer layers which leave residue on the graphene that is very hard to remove completely.[24,26] Consequently, the surface contaminants play a major role in the subsequent physical properties of graphene and distort its electrochemical response.[23,27–29]

Due to these complications in the fabrication of graphene electrodes, and the resultant variability in electrode response, the electrochemical activity of graphene is still controversial. A perfect graphene surface exposes only the pristine hexagonal lattice of sp^2 carbon atoms to solution; in the terminology used to describe graphite, this is known as the basal plane. However, defects are likely to have significantly different electrochemical activity. The most prominent type of defect for isolated graphene sheets are the edges; similar in structure to edge plane graphite but only a monolayer thick. For continuous layers of CVD graphene, the analogous defects are the grain boundaries, although these contain defects without dangling bonds. Some reports claim that only the defects / edges of graphene are electrochemically active,[18,30] whilst others claim that the basal plane is also active.[23,29] This is also a matter of debate for HOPG, despite decades of electrochemical investigations.[31–34] Added to that, changes in electrode activity upon exposure to air and the controversial role of surface contaminants make it hard to unambiguously determine the true electrochemical activity of HOPG and graphene.[23,34–36] Despite this, graphite and graphene based electrodes are widely applied, with or without further modification. Hence a simple but reproducible and well-characterised source of graphene electrodes would be of great use for developing our understanding of the fundamental electrochemistry of these materials, and testing and refining applications.

Here we show, for the first time, how electrochemical measurements can easily, quickly and reproducibly be made using pristine CVD graphene grown on copper (CVD-Gr) without post treatment of the graphene on copper substrate. We find fast electron transfer kinetics for both inner sphere and outer sphere redox probes, even for monolayer CVD-Gr on copper with graphene grain sizes of ~ 50 μm. Study of partially covered samples, and samples of different graphene grain size, suggests that in this instance the electrochemical response is dominated by basal plane graphene. The ease of fabrication, stability and reproducibility suggest that graphene on copper shows great promise as a model electrode.

Experimental

Low-pressure CVD of graphene on copper. Graphene was grown on copper foil using a low-pressure CVD system as described previously.[37] In brief, copper foil substrates (99.5% purity, 0.025 mm thick, Alfa Aesar product number 13382) were cleaned by electrochemical polishing and washing, following the procedure described by Miseikis et al.[38] Using a 1 inch tube furnace pumped to low pressure by a turbomolecular pump, the foil was heated to 1000 °C and annealed for 20 minutes prior to growth. A hydrogen flow was maintained throughout the process, with methane introduced for the growth stage. The standard growth conditions used were 10 standard cubic centimetres (sccm) of hydrogen, with 2 sccm of methane and a growth time of 30 minutes. For partial coverage samples the growth time was reduced to 25 minutes. For smaller domain samples the methane flow rate was increased to 10 sccm and the growth time reduced to 10 minutes. After cooling to room temperature, the graphene on copper samples were removed from the furnace and stored under ambient conditions before use.

Raman spectroscopy and scanning electron microscopy (SEM). Raman spectra were recorded with a Rainshaw InVia micro-Raman system using a 514 nm laser excitation, with a laser power of *ca.* 5mW. A confocal microscope with 50x lens was used to record spectra at a spatial resolution of ~2 μm. SEM characterization was performed on a ZEISS Supra 55-VP field emission SEM, operated at 10 kV, using the in lens secondary electron detector. Raman and SEM analysis were performed on the graphene on copper foils as grown. ImageJ[39] was used to analyse the SEM images and quantify the coverage of the samples (see Figure SI3).

Transmission electron microscopy (TEM). Bright-field images, electron diffraction patterns and dark-field images were acquired on a Jeol 2000FX operated at 200 kV with a Gatan Orius camera. For TEM analysis, the graphene was transferred from the copper growth substrate to a conventional TEM grid (Agar Scientific Hexagonal 600 mesh Copper 3.05mm thick). A thin amorphous carbon film was evaporated on top of the graphene on copper, a thin layer of formvar was spin coated on top of that, and then the copper was removed with an ammonium persulphate etchant (5.7 g of ammonium persulphate dissolved in 100 mL of water). After etching, the formvar/amorphous carbon/graphene stack was repeatedly washed by transferral to deionised water and then transferred to the TEM grid. Finally, the formwar was removed by immersing the grid in chloroform. To prevent tearing of the remaining film as a result of the high surface tensions caused by evaporative drying, the grid was then transferred to an intermediate acetone flask before being dried using a critical point dryer.

Scanning tunnelling microscopy (STM) and atomic force microscopy (AFM). STM images were acquired in ambient conditions with a Multimode STM with Nanonis controller using mechanically sheared PtIr tips. AFM images were acquired in AC (tapping) mode using an Asylum Research MFP-3D-SA.

Electrochemical measurements. Cyclic voltammograms (CVs) were recorded in a three-electrode configuration using a BST8-stat instrument from MTI KJ group. The as-made CVD-Gr on copper was used as the working electrode. To achieve a constant surface area for the electrode, each sample was masked with a piece of 3M Model 470 Electroplater'tape with a pre-cut 0.05 cm^2 hole. A GAMRY electrochemical cell (model PTC1 paint test cell) was clamped to the working electrode (see SI 1). A GAMRY Ag/AgCl (in saturated KCl) reference electrode and Pt wire counter electrode were used.

Solutions. All chemicals were used as received. Aqueous solutions were prepared using high purity water. For cyclic voltammetry measurements, either potassium hexacyanoferrate (II) trihydrate 99% (Sigma-Aldrich) in a supporting electrolyte of potassium carbonate (Fisher Scientific) or Hexaammineruthenium (III) chloride 98% (Sigma-Aldrich) in a supporting electrolyte of potassium nitrate (Sigma-Aldrich) were typically used.

Results and discussion

Graphene on copper growth and characterisation

Graphene was grown on copper foil by low pressure chemical vapour deposition, as described in the experimental section. Figure 1a shows a typical SEM image of one of the standard graphene on copper substrates (CVD-Gr) used here. The dark lines are wrinkles in the graphene formed during cooling due to the difference in thermal expansion coefficients between graphene and copper; otherwise the contrast is uniform indicating continuous monolayer coverage. Further SEM images are shown in supporting information (see SI 2). From these SEM images, the surface coverage of the graphene on copper is measured to be > 99 %, of which > 95 % is monolayer. This is consistent across CVD-Gr samples grown under the same conditions. With shorter growth times (see experimental), an incomplete film is formed and isolated graphene islands can be seen, resulting in only partial coverage of the copper surface. From images of such samples, and dark-field TEM and electron diffraction of full coverage samples (see supporting information Figure SI4), the average graphene grain size is measured to be ~ 50 µm under these growth conditions.

The quality of the grown graphene was assessed by Raman spectroscopy in-situ on the copper substrate. As evidenced in Figure 1b, a typical Raman spectrum for this material shows single peaks for the G and the 2D bands at *ca.* 1580 cm^{-1} and 2690 cm^{-1}, respectively.[40] There is no apparent D peak (expected at 1350 cm^{-1}). Moreover, the sharpness of the G and the 2D bands, and the ratio between their intensities (I_{2D}/I_G ~ 4) confirm that the sample is mainly composed of high quality single layers of graphene.[40] Scanning tunneling microscopy (STM) shows that CVD-Gr samples are clean (see supporting information Figure SI 5), even after prolonged exposure to atmosphere, with atomic resolution imaging revealing the characteristic hexagonal structure of graphene. The absence of a D peak in the Raman spectra, and the STM images, indicate no defects on the basal plane. With a grain size of ~ 50 µm, the ratio of basal plane carbon atoms to grain boundary carbon atoms is ~ 10^5, i.e. only ~0.001 % of the carbon atoms are at the grain boundaries. This corresponds to a grain boundary density of ~ 0.02 µm $µm^{-2}$ (in analogy to the step density referred to for

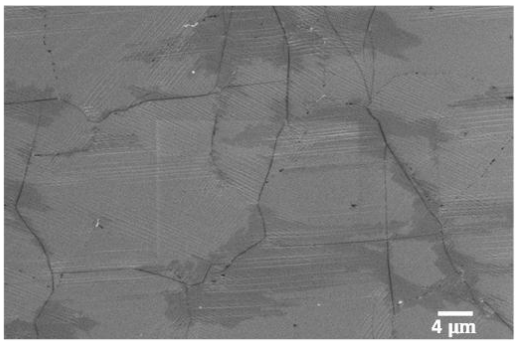

(a)

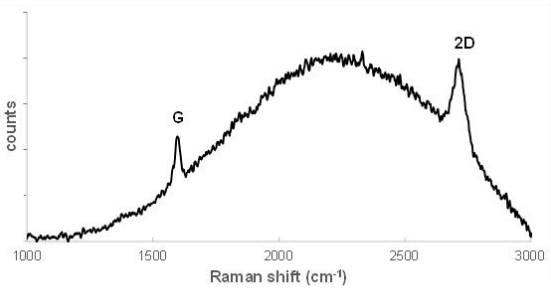

(b)

Figure 1. a) SEM image of the as-made CVD grown graphene on copper foil, CVD-Gr. b) Raman spectrum of a CVD-Gr working electrode, recorded at 514 nm excitation wavelength.

HOPG,[34] by comparison to which this corresponds to the highest grade HOPG).

The as grown CVD-Gr was used without modification as a working electrode for electrochemical investigations (for the experimental set-up refer to the experimental section and to SI1).

Electrochemical activity with respect to inner and outer sphere species.

Most electrochemical studies of graphene use a standard KCl supporting electrolyte.[34,41] However, this is inadvisable when using a copper substrate as KCl rapidly corrodes copper. During the electrochemical experiment, first, Cu^+ reacts with Cl^- giving rise to cuprous chloride (CuCl). In a second step the CuCl formed reacts with water to produce cuprous oxide, which is then oxidised to cupric hydroxide ($Cu(OH)_2$), atacamite ($Cu_2(OH)_3Cl$) and/or malachite ($CuCO_3$ $Cu(OH)_2$).[42] This results in a green deposit on the copper electrodes (SI 6a), which occurs even if only small regions of copper are exposed,

and hence damages and fouls the graphene on copper electrodes. As a result, KCl supporting electrolytes should be avoided whilst studying the electrochemistry of graphene on copper. Instead, K_2CO_3 supporting electrolyte can be used at positive potentials (reacts with copper at negative potentials) and KNO_3 at negative potentials (reacts with copper at positive potentials) (SI 6b and SI6c).

We first investigated the electrochemical properties of CVD-Gr with respect to a surface sensitive inner-sphere redox couple,[5] 1 mM potassium ferrocyanide (II) ($[Fe(CN)_6]^{4-}$) in 0.5 M K_2CO_3. A typical cyclic voltammogram (CV) from a CVD-Gr working electrode is shown in Figure 2a, where well defined peaks are observed for the reduction and oxidation processes, having a peak to peak separation of 68.6 mV at 0.1 V s^{-1}, which points to a quasi-reversible process.[43] For comparison, Figure 2a also shows a CV taken under similar conditions using a copper foil electrode without graphene: the CV is drawn out without clear redox peaks, consistent with much slower electron transfer kinetics. Given that > 99% of the CVD-Gr electrode surface is covered in graphene, and that the exposed copper is thus shown to have slower electron transfer kinetics, it is clear that the observed electrochemical response for the CVD-Gr electrodes is due to graphene.

Figure 2b shows CVs with an outer-sphere redox probe,[5] 1 mM hexaammineruthenium (III) chloride ($[Ru(NH_3)_6]^{3+}$) in KNO_3 0.5 M. As also shown in Figure 2b, CVs from bare copper under the same conditions gave only very low currents, excluding the copper substrate as the source of the electrochemical activity (note that the exposed copper surface rapidly oxidises to insulating copper oxide on exposure to air). Hence, unlike for CVD grown graphene on nickel,[16] the electrochemical response of the CVD-Gr working electrodes under these conditions are dominated by the graphene overlayer rather than the underlying substrate.

It is interesting to note that for both redox couples, the CVs were reproducible and stable. After 50 consecutive CVs the change in peak reduction current for both redox couples at 1 mM concentration was *ca.* 5 % (see SI 7). AFM topographic maps after such repeated cycling showed no evidence of any contamination for $[Ru(NH_3)_6]^{3+}$ and only small isolated adsorbates for $[Fe(CN)_6]^{4-}$ (see SI6). The electrochemical response was consistent across many similarly grown CVD-Gr samples, and did not depend on the length of time since growth (from a few hours to a few weeks) despite being stored under ambient conditions. This is in marked contrast to HOPG.[29] It is usual to cleave HOPG immediately prior to use for electrochemistry as the surface is rapidly contaminated, blocking and reducing the electrochemical activity (similarly it is usual to cleave HOPG immediately prior to STM, but does not seem to be necessary for CVD-Gr). In addition, the electrochemical activity of inner sphere redox couples such as $[Fe(CN)_6]^{4-}$ has been highly controversial with a report by Patel et al. showing that the $[Fe(CN)_6]^{4-}$ rapidly adsorbs to HOPG, blocking the electrochemical activity and dramatically slowing the electron transfer kinetics. [34] The CVD-Gr electrodes thus seem to be less prone to contamination or fouling than HOPG.

Electron transfer kinetics.

More detailed insight into the electron transfer kinetics can be gained by studying the effect of varying the scan rate. Figure 3 shows typical cyclic voltammograms at scan rates from 0.01 to 0.08 V s^{-1} for $[Ru(NH_3)_6]^{3+}$ and $[Fe(CN)_6]^{4-}$. At low scan rates, up to around 0.1 V s^{-1}, a linear relationship is observed between the intensity of the forward peak and the square root of the scan rate (Figure 3a (i), *inset,* and Figure 3b (i), *inset*), suggesting diffusion-controlled voltammetric responses for both redox couples. Using the Randles-Sevcik equation,[43] the diffusion coefficient was calculated to be $D = (1.5 \pm 0.2) \times 10^{-5}$ cm^2 s^{-1} for $[Ru(NH_3)_6{}^{3+}]$ and $D = (0.6 \pm 0.1) \times 10^{-5}$ cm^2 s^{-1} for $[Fe(CN)_6{}^{4-}]$ (SI8 and SI9), both in good agreement with previous reports.[34,44]

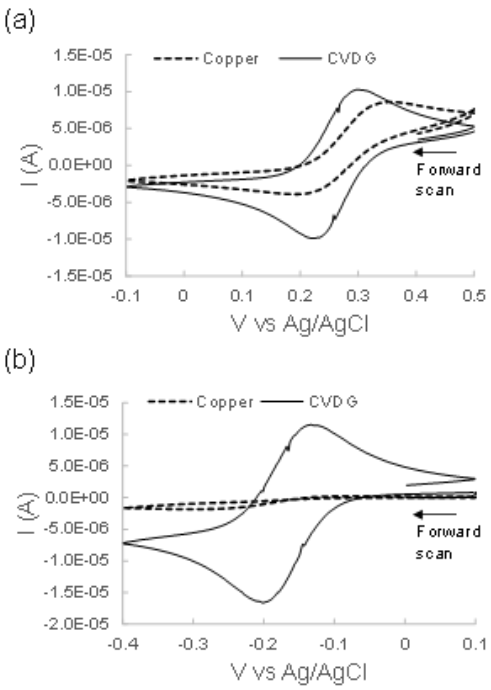

Figure 2. Cyclic voltammograms at 0.1 V s^{-1} for the oxidation of (a) 1 mM $[Fe(CN)_6]^{4-}$ in 0.5M K_2CO_3 and (b) 1 mM $[Ru(NH_3)_6]^{3+}$ in 0.5 M KNO_3, using copper foil (dashed line) and CVD-Gr (solid line) as working electrodes. In all the cases, the measurements were taken over electrodes with a constant surface area of 0.05 cm^2 (see experimental section and SI 1)

At higher scan rates the response becomes kinetically controlled. The potential difference between the oxidation and reduction peaks (ΔE_p) as a function of the scan rate, as shown in Figure 3a (ii), varies between 60 mV and 166 mV for $[Fe(CN)_6]^{4-}$ from 0.01 to 10 V s^{-1}, and between 66 mV and 250 mV for the corresponding scan rates for $[Ru(NH_3)_6]^{3+}$. For both redox couples, ΔE_p increases with increasing scan rate and demonstrates quasi-reversible behaviour (for which ΔE_p = 59 mV is expected)[43] at low scan rates. Following Nicholson's semi-empirical approach,[45,46] the ΔE_p values in the range 80-140 mV can be converted into a dimensionless kinetic parameter ψ that is directly proportional to the inverse of the square root of the scan rate, $\upsilon^{-1/2}$:

$$\psi = k^\circ \sqrt{\frac{RT}{\pi n F D}}\, U^{-1/2}$$

where $k°$ is the heterogeneous rate transfer constant, n = 1 is the number of electrons involved in the redox reaction, F is the Faraday constant and D is the diffusion coefficient. Hence, the transfer rate constant $k°$ can be determined from a linear fit of ψ vs $U^{-1/2}$ (Figures 3a (iii) and 3b (iii)). From the slope, we found $k°$ = 0.0140 ± 0.0005 cm s^{-1} for $[Fe(CN)_6]^{4-}$ and $k°$ = 0.012 ± 0.001 cm s^{-1} for $[Ru(NH_3)_6]^{3+}$. The signal appeared to be highly reproducible over all the tested samples (*i.e.* at least five samples for each redox couple); the quoted uncertainty in $k°$ reflects the standard deviation in $k°$ across the tested samples and hence demonstrates the reproducibility.

To put this into context, it is worth comparing these values with other reported transfer rate constants. Typical reported values for graphene are much lower. For example, for ferrocenemethanol redox couple with a graphene monolayer on a silicon wafer a value of $k°$ = 0.0012 cm s^{-1} was reported.[15] By comparison with graphite, the transfer rate constant is again higher here, e.g. edge-plane pyrolytic graphite (EPPG; $k°$ = 0.0026 cm s^{-1})[47] and basal-plane pyrolytic graphite (BPPG; $k°$ = 0.00033 cm s^{-1}), for potassium ferrocyanide redox couple.[47] However, single walled carbon nanotubes have been shown to have faster transfer rate constants, of up to 1-10 cm s^{-1},[48] and also HOPG can show faster electron transfer before ageing.[35] It is interesting that fast and comparable rate constants were obtained for both $[Fe(CN)_6]^{4-}$ and $[Ru(NH_3)_6]^{3+}$. Some previous reports have claimed that the basal surface of sp^2 materials is inert in terms of electron transfer, and thus, a big difference between employing inner- (classified as surface sensitive) and outer-sphere redox probes (classified as surface insensitive) should be observed,[16,47] which is clearly not supported by this data. Again it is worth noting that the grain size of graphene

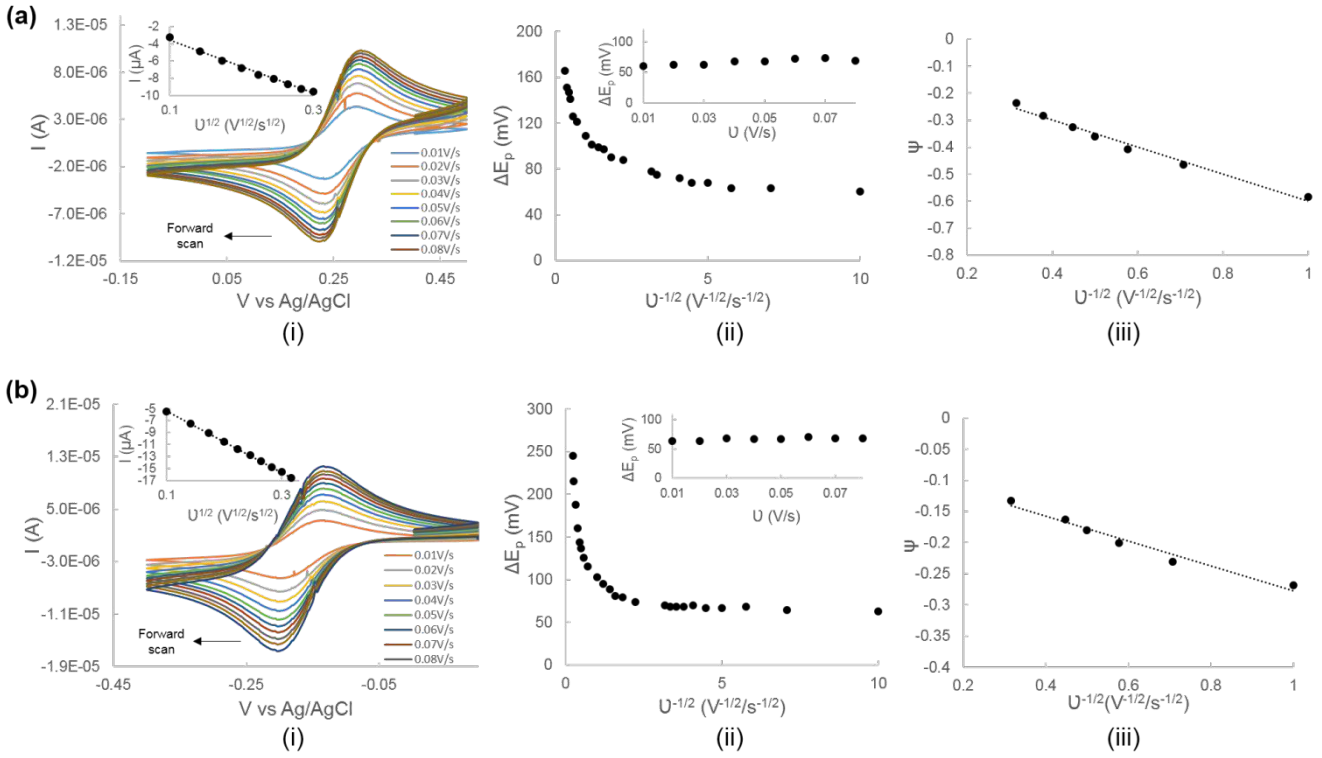

Figure 3. (i) CVs at a range of scan rates for the oxidation of (a) 1 mM $[Fe(CN)_6]^{4-}$ in 0.5 M K_2CO_3 and (b) 1 mM $[Ru(NH_3)_6]^{3+}$ in 0.5 M KNO_3, using CVD-Gr on copper as working electrode. In the inset the linear dependency of the peak current as a function (scan rate)$^{1/2}$ is shown. (ii) Peak to peak separation (ΔE_p) as a function of the (scan rate)$^{-1/2}$. In the inset, a constant ΔE_p value is shown for low scan rates. (iii) Kinetic parameter (ψ) against (scan rate)$^{-1/2}$. From the fitting the rate constant can be calculated.

Table 1. Summary of electrochemical parameters at a CVD-Gr working electrode for the inner- and outer-sphere redox probes studied.

CVD-Gr on copper				
	ΔE_p (mV) at (0.01-0.1)V s^{-1}	$E_{1/2}$ (V)	D (10^{-5}cm^2 s^{-1})	$k°$ (cm s^{-1})
$[Fe(CN)_6]^{4-}$, KNO_3	69 ± 1	0.265	0.6 ± 0.1	0.0140 ±0.0005
$[Ru(NH_3)_6]^{3+}$, K_2CO_3	67 ± 1	0.165	1.5 ± 0.2	0.012 ± 0.001

Journal Name

ARTICLE

here was around 50 µm, so that the ratio of basal plane graphene atoms to grain boundary carbon atoms is around 10^5. There are small regions with two or more layers (evident in the SEM images), but these make up less than 5 % of the area and the extra layers are under the first so that no edges are exposed.[49] It is possible that the wrinkles (again evident in the SEM images, and with a density of around 0.08 µm µm^{-2}) are more electrochemically active due to their high curvature, in analogy to the high electrochemical activity of single walled carbon nanotubes. However, as discussed later this does not seem to be the case.

The effect of the metal substrate should also be considered. Angle resolved photoemission spectroscopy has shown that CVD grown graphene on copper foil has an electronic structure that is effectively decoupled from the copper surface and hence the density of states,[37] which to a certain extent dictates the electrochemical activity, is the same as for isolated graphene. From this regard, the CVD-Gr electrodes would be expected to be representative of graphene. However, the effect of water on graphene on copper is less clear. Density functional theory has shown that water adsorbs more strongly on metal supported graphene,[50] whilst the question of whether graphene on copper is wetting transparent (i.e. is the wettability of graphene on copper determined by the graphene or the underlying substrate) is still under debate.[51,52] It is, however, clear that the chemical reactivity and electrochemical activity of graphene is always to some extent dependent on the substrate.[53,54] For instance, changes in the local curvature and local charge, as are common for graphene on e.g. silicon oxide, affect the electronic structure of graphene and hence its reactivity. In that regard, graphene on copper is a well-defined model as the surface is locally atomically flat and the underlying copper surface gives a uniform electrostatic background.

Effect of partial graphene coverage and varying graphene grain size.

Finally we study whether the electrochemical behavior of graphene on copper is dependent on (i) the amount of exposed copper substrate and (ii) the size of the graphene grains. To test this, the CVD growth conditions were changed to grow two new types of sample, shown in Figure 4 and as described in the experimental section. For the first type of sample, the growth time was decreased such that growth finished before a continuous graphene film was formed, forming a partially covered surface with regions of copper exposed (CVD-Gr-exp). For the second, higher flow rates of methane were used to increase the nucleation density and hence form smaller graphene grain sizes (CVD-Gr-sg). Figure 4 shows SEM images of the three types of tested samples, with further images in supporting information (SI 10). From these SEM images we estimate the grain size for CVD-Gr-exp to be around 50µm, with 90 % coverage of graphene of which 97 % is monolayer. Similarly for CVD-Gr-sg we find the typical grain sizes to be 3 to 15 µm with *ca.* 85 % coverage of graphene of which 90 % is monolayer. For partially covered graphene on copper, wrinkles do not form on cooling and the edges of the islands are no longer grain boundaries but instead more analogous to edge plane graphite. Decreasing the coverage of graphene decreases the fraction of basal plane graphene; decreasing the island size at the same coverage increases the proportion of edge plane graphene. As such, studying the effect of coverage and island size can give some insight into the origin of the graphene electrochemical activity.

Figure 4 and SI11 compare CVs on CVD-Gr with CVD-Gr-exp and CVD-Gr-sg for $[Ru(NH_3)_6]^{3+}$ and $[Fe(CN)_6]^{4-}$, respectively. When using the outer-sphere redox probe $[Ru(NH_3)_6]^{3+}$, no significant changes are observed for CVD-Gr-exp compared to CVD-Gr; a diffusion coefficient of D = 2.22 × 10^{-5} cm^2 s^{-1} and a rate constant of $k°$ = 0.009 cm s^{-1} are calculated from the scan rate dependence of the CVs, using the methodology described earlier. Note that these values are calculated assuming a reversible diffusion / kinetic limited current respectively, and that may not be the case for these samples with exposed copper. However, the small decrease in the rate constant when compared to CVD-Gr (0.009 cm s^{-1} vs 0.012 cm s^{-1}, respectively) can be explained in terms of the decrease of active material (*i.e.* graphene). As shown in Figure 2, the copper surface is inactive to $[Ru(NH_3)_6]^{3+}$, so the partially covered sample is analogous to a partially blocked electrode and the measured electron transfer rate constant should scale with the active area.[55] We note that the amount of 'edge plane' graphene (graphene grain boundaries or graphene island edges) is increased in this sample compared to the fully covered sample (~ 0.5 µm µm^{-2} for fully covered compared to ~ 0.1 µm µm^{-2} for CVD-Gr-exp) and there are no wrinkles present.

Comparison between the electrochemical activity of CVD-Gr and CVD-Gr-sg against $[Ru(NH_3)_6]^{3+}$ also shows little difference. From the CVs, a diffusion coefficient of D = 2.22 × 10^{-5} cm^2 s^{-1} and a rate constant of $k°$ = 0.009 cm s^{-1} were calculated, which are comparable to the values obtained for CVD-Gr and CVD-Gr-exp (Table 2). Here, the 'edge plane' graphene is increased further (to ~ 0.5 µm µm^{-2}).

Analysing these results, we see that the rate transfer constant roughly scales with graphene coverage but is not strongly correlated to the amount of 'edge plane' graphene or wrinkles, see Table 2. Therefore, our results suggest that basal-plane

graphene is electrochemically active and, in this case at least, seems to dominate the electrochemical activity. This is in agreement with recent reports on HOPG[23] but contradicts other reports which claim negligible electrochemical activity of the basal-plane of graphene.[18,30]

We note that when the surface is only partially covered with graphene, significant changes in the electrochemical behaviour are observed when using the inner sphere $[Fe(CN)_6]^{4-}$. As shown in SI11, the background current increases, which is accompanied by a change in the shape of the CV. This behaviour can be attributed to the exposed copper, and complicates quantitative investigation of the kinetics. For comparison, the electrochemistry of a clean copper foil was studied against $[Fe(CN)_6]^{4-}$ at different scan rates. As shown in SI12, at high scan rates the electrochemical response is similar to that shown by CVD-Gr-exp and CVD-Gr-sg. Moreover, in contrast to CVD-Gr, the electrochemical response of the copper foil changes with successive cycling in $[Fe(CN)_6]^{4-}$ (SI12) but remains constant when cycling in $[Ru(NH_3)_6]^{3+}$ (SI13). The change in shape of the CV and changes over time suggest that adsorption is occurring, this is confirmed by SEM images (SI12b) taken after cycling. Qualitative comparison between the electrochemical activities can be made by measuring the peak to peak separation of the response on top of this background, as shown in Table SI 11. The similarity in the peak to peak separations as a function of scan rate for the different types of sample suggests that the electron transfer kinetics are also similar for the $[Fe(CN)_6]^{4-}$ redox couple, as quantitatively shown in Table 2 for $[Ru(NH_3)_6]^{3+}$. This is despite the orders of magnitude changes in wrinkle density, grain size and 'edge-plane' density. This suggests that here the electrochemical response is dominated by the graphene basal plane, even for the inner sphere $[Fe(CN)_6]^{4-}$ redox couple. It should be noted that even though outer- and inner-sphere redox probes can be employed for studying the electrochemistry of CVD-Gr on copper, accurate quantification of the kinetics is only easily achievable with electrolytes and redox couples that do not readily react or adhere to any exposed copper surface.

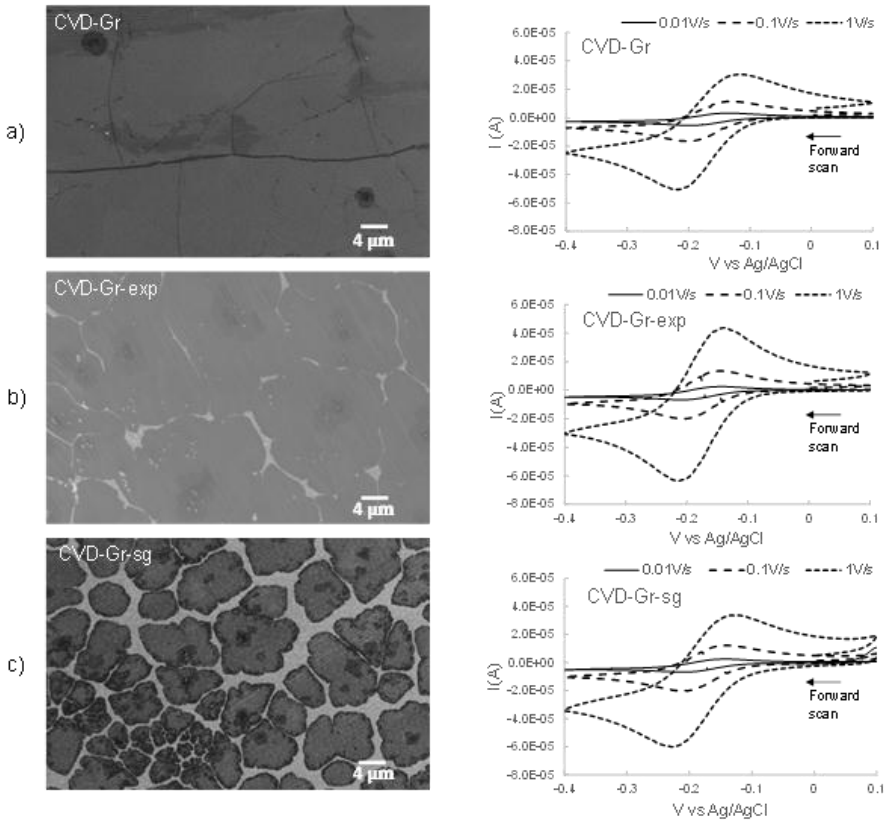

Figure 4. SEM images and representative CVs against $[Ru(NH_3)_6]^{3+}$ at 0.01V s^{-1} (solid line), 0.1V s^{-1} (dashed lines) and 1V s^{-1} (dotted line) for (a) CVD-Gr, (b) CVD-Gr-exp and (c) CVD-Gr-sg working electrodes.

Table 2. Summary of the kinetic parameters obtained against $[Ru(NH_3)_6]^{3+}$ for the three working electrodes tested CVD-Gr, CVD-Gr-exp and CVD-Gr-sg

$[Ru(NH_3)_6]^{3+}$						
	% Coverage	Grain Size	'Edge-plane'* (µm µm^{-2})	Wrinkles (µm µm^{-2})	$k°$ (cm s^{-1})	D (10^{-5} cm^2 s^{-1})
CVD-Gr	> 99%	~ 50 µm	0.05	0.08	0.012±0.001	1.49 ± 0.2
CVD-Gr-exp	~ 90%	~ 50 µm	0.1	-	0.009	2.22
CVD-Gr-sg	~ 85%	3 to 15 µm	0.5	-	0.009	2.22

Journal Name

ARTICLE

Conclusions

Our results demonstrate that electrochemical experiments can be directly performed using CVD grown graphene on copper without further treatment provided appropriate electrolytes are used, avoiding transfer or etching of the underlying substrate which can damage the graphene and increase contaminants. CVD-Gr on copper shows a fast kinetic response against both inner- and outer-sphere redox couples, which contrasts with some previous works carried out on monolayer graphene on silicon oxide, edge-plane pyrolytic graphite, and basal-plane pyrolytic graphite. Its electrochemical response is reproducible and stable even for inner sphere redox couples, unlike previous reports for HOPG.

Changing the surface coverage of graphene and the size of the graphene grains showed that the heterogeneous electron transfer rate constant of the electrode is strongly correlated to percentage of the surface covered by graphene but not to the amount of 'edge plane' graphene present. This suggests that, for the case of fully covered graphene on copper at least, the electrochemical response is dominated by the electrochemical activity of the basal plane of graphene.

The CVD-Gr electrodes are quick and easy to prepare and give stable and reproducible results. They are thus a convenient platform for studying electrochemical properties of graphene electrodes and the effects of covalent and noncovalent functionalization.

Acknowledgements

CBN acknowledges support from her fellowship from the Vali+D program of the Generalitat Valenciana (Spain). We thank Alexander Marsden and Julie Macpherson for helpful suggestions. ZPLL thanks the EPSRC for support through a studentship (EP/M506679/1).

References

1 D. Chen, H. Feng and J. Li, *Chem. Rev.*, 2012, **112**, 6027–53.
2 C. N. R. Rao, K. Biswas, K. S. Subrahmanyam and a. Govindaraj, *J. Mater. Chem.*, 2009, **19**, 2457.
3 Y. Zhu, S. Murali, W. Cai, X. Li, J. W. Suk, J. R. Potts and R. S. Ruoff, *Adv. Mater.*, 2010, **22**, 3906–3924.
4 D. a C. Brownson and C. E. Banks, *Phys. Chem. Chem. Phys.*, 2012, **14**, 8264–8281.
5 D. a C. Brownson, D. K. Kampouris and C. E. Banks, *Chem. Soc. Rev.*, 2012, **41**, 6944–6976.
6 C. N. R. Rao, a K. Sood, K. S. Subrahmanyam and A. Govindaraj, *Angew. Chemie Int. ed.*, 2009, **48**, 7752–7777.
7 C. Bosch-Navarro, E. Coronado, C. Marti-Gastaldo, J. F. Sanchez-Royo and M. G. Gomez, *Nanoscale*, 2012, **4**, 3977–3982.
8 H. R. Thomas, S. P. Day, W. E. Woodru, C. Valle, R. J. Young, I. A. Kinloch, G. W. Morley, J. V Hanna, N. R. Wilson and J. P. Rourke, *Chem. Mater.*, 2013, **25**, 3580–3588.
9 J. P. Rourke, P. Pandey, J. J. Moore, M. Bates, I. Kinloch, R. J. Young and N. R. Wilson, *Angew. Chem. Int. Ed. Engl.*, 2011, **50**, 3173–3177.
10 Y. Hernandez, V. Nicolosi, M. Lotya, F. M. Blighe, Z. Sun, S. De, I. T. McGovern, B. Holland, M. Byrne, Y. K. Gun'Ko, J. J. Boland, P. Niraj, G. Duesberg, S. Krishnamurthy, R. Goodhue, J. Hutchison, V. Scardaci, A. C. Ferrari and J. N. Coleman, *Nat. Nanotechnol.*, 2008, **3**, 563–568.
11 K. S. Novoselov, A. K. Geim, S. V. Morozov, D. Jiang, Y. Zhang, S. V. Dubonos, I. V. Grigorieva and A. A. Firsov, *Science*, 2004, **306**, 666–669.
12 Y. Zhang, L. Zhang and C. Zhou, *Acc. Chem. Res.*, 2013, **46**, 2329–2339.
13 N. Petrone, C. R. Dean, I. Meric, A. M. Van Der Zande, P. Y. Huang, L. Wang, D. Muller, K. L. Shepard and J. Hone, *Nano Lett.*, 2012, **12**, 2751–2756.
14 M. Pumera, *Electrochem. commun.*, 2013, **36**, 14–18.
15 W. Li, C. Tan, M. A. Lowe, H. D. Abruna and D. C. Ralph, *ACS Nano*, 2011, **5**, 2264–2270.
16 D. a C. Brownson and C. E. Banks, *Phys. Chem. Chem. Phys.*, 2011, **13**, 15825–15828.
17 A. Gutés, C. Carraro and R. Maboudian, *Biosens. Bioelectron.*, 2012, **33**, 56–59.
18 D. a C. Brownson, S. a Varey, F. Hussain, S. J. Haigh and C. E. Banks, *Nanoscale*, 2014, **6**, 1607–1621.
19 A. Ambrosi, A. Bonanni, Z. Sofer and M. Pumera, *Nanoscale*, 2013, **5**, 2379–2387.
20 J. Zhong, J. Zhang, X. Jin, J. Liu, Q. Li, M. Li, W. Cai, D. Wu, D. Zhan and B. Ren, *J. Am. Chem. Soc.*, 2014, **136**, 16609–16617.
21 J. Zhong, J. Liu, Q. Li, M.-G. Li, Z.-C. Zeng, S. Hu, D. Wu, W. Cai and B. Ren, *Electrochim. Acta*, 2013, **110**, 754–761.
22 N. L. Ritzert, J. Rodríguez-López, C. Tan and H. D. Abruña, *Langmuir*, 2013, **29**, 1683–1694.
23 H. V Patten, V. M, N. Clark, C. A. Muryn, I. A. Kinloch and R. A. W. Dryfe, *Faraday Discuss.*, 2014, **172**, 261–272.
24 J. W. Suk, W. H. Lee, J. Lee, H. Chou, R. D. Piner, Y. Hao, D. Akinwande and R. S. Ruoff, *Nano Lett.*, 2013, **13**, 1462–1467.
25 A. Ambrosi and M. Pumera, *J. Phys. Chem. C*, 2013, **117**, 2053–2058.
26 C. J. Shih, Q. H. Wang, S. Lin, K. C. Park, Z. Jin, M. S. Strano and D. Blankschtein, *Phys. Rev. Lett.*, 2012, **109**, 1–5.
27 A. Ambrosi and M. Pumera, *Nanoscale*, 2014, **6**, 472–476.
28 C. Tan, J. Rodríguez-López, J. J. Parks, N. L. Ritzert, D. C. Ralph and H. D. Abruña, *ACS Nano*, 2012, **6**, 3070–3079.
29 M. Velicky, D. F. Bradley, A. J. Cooper, E. W. Hill, I. A. Kinloch, A. Mishchenko, K. S. Novoselov, H. V Patten, P. S. Toth, A. T. Valota, S. D. Worrall and R. A. W. Dryfe, *ACS Nano*, 2014, **8**, 10089–10100.
30 W. Yuan, Y. Zhou, Y. Li, C. Li, H. Peng, J. Zhang, Z. Liu, L. Dai and G. Shi, *Sci. Rep.*, 2013, **3**, 2248.
31 R. J. Bowling, R. T. Packard and R. L. McCreery, *J. Am. Chem. Soc.*, 1989, **111**, 1217–1223.
32 C. E. Banks, T. J. Davies, G. G. Wildgoose and R. G. Compton, *Chem. Commun.*, 2005, 829–841.

33 X. Ji, C. E. Banks, A. Crossley and R. G. Compton, *ChemPhysChem*, 2006, **7**, 1337–1344.
34 A. N. Patel, M. G. Collignon, M. A. O. Connell, W. O. Y. Hung, K. Mckelvey, J. V Macpherson and P. R. Unwin, *J. Am. Chem. Soc.*, 2012, **134**, 20117–20130.
35 A. G. Güell, A. S. Cuharuc, Y.-R. Kim, G. Zhang, S. Tan, N. Ebejer and P. R. Unwin, *ACS Nano*, 2015, **9**, 3558–3571.
36 K. K. Cline, M. T. Mcdermott and R. L. Mccreery, *J. Phys. Chem.*, 1994, **98**, 5314–5319.
37 N. R. Wilson, A. J. Marsden, M. Saghir, C. J. Bromley, R. Schaub, G. Costantini, T. W. White, C. Partridge, A. Barinov, P. Dudin, A. M. Sanchez, J. J. Mudd, M. Walker and G. R. Bell, *Nano Res.*, 2013, **6**, 99–112.
38 V. Miseikis, D. Convertino, N. Mishra, M. Gemmi, T. Mashoff, S. Heun, N. Haghighian, F. Bisio, M. Canepa, V. Piazza and C. Coletti, *2D Mater.*, 2015, **2**, 014006.
39 C. A. Schneider, W. S. Rasband and K. W. Eliceiri, *Nat. Methods*, 2012, **9**, 671–675.
40 A. C. Ferrari, *Solid State Commun.*, 2007, **143**, 47–57.
41 A. T. Valota, I. a Kinloch, K. S. Novoselov, C. Casiraghi, A. Eckmann, E. W. Hill and R. a W. Dryfe, *ACS Nano*, 2011, **5**, 8809–8815.
42 G. Kear, B. D. Barker and F. C. Walsh, *Corros. Sci.*, 2004, **46**, 109–135.
43 C. G. Zoski, *Handbook of Electrochemistry*, Elsevier, 2007.
44 S. J. Konopka and B. McDuffie, *Anal. Chem.*, 1970, **42**, 1741–1746.
45 R. S. Nicholson, *Anal. Chem.*, 1965, **37**, 1351–1355.
46 R. S. Nicholson, *Anal. Chem.*, 1964, **38**, 1406.
47 K. Griffiths, C. Dale, J. Hedley, M. D. Kowal, R. B. Kaner and N. Keegan, *Nanoscale*, 2014, **6**, 13613–13622.
48 P. V. Dudin, M. E. Snowden, J. V. MacPherson and P. R. Unwin, *ACS Nano*, 2011, **5**, 10017–10025.
49 S. Nie, W. Wu, S. Xing, Q. Yu, J. Bao, S. S. Pei and K. F. McCarty, *New J. Phys.*, 2012, **14**, 093028.
50 X. Li, J. Feng, E. Wang, S. Meng, J. Klime and A. Michaelides, *Phys. Rev. B*, 2012, **85**, 085425.
51 C.-Y. Lai, T.-C. Tang, C. a. Amadei, A. J. Marsden, A. Verdaguer, N. Wilson and M. Chiesa, *Carbon*, 2014, **80**, 784–792.
52 J. Rafiee, X. Mi, H. Gullapalli, A. V Thomas, F. Yavari, Y. Shi, P. M. Ajayan and N. a Koratkar, *Nat. Mater.*, 2012, **11**, 217–222.
53 P. Szroeder, N. G. Tsierkezos, M. Walczyk, W. Strupiński, A. Górska-Pukownik, J. Strzelecki, K. Wiwatowski, P. Scharff and U. Ritter, *J. Solid State Electrochem.*, 2014, **18**, 2555–2562.
54 Q. H. Wang, Z. Jin, K. K. Kim, A. J. Hilmer, G. L. C. Paulus, C.-J. Shih, M.-H. Ham, J. D. Sanchez-Yamagishi, K. Watanabe, T. Taniguchi, J. Kong, P. Jarillo-Herrero and M. S. Strano, *Nat. Chem.*, 2012, **4**, 724–732.
55 C. Amatore, J. M. Saveant and D. Tessier, *J. Electroanl. Chem*, 1983, **147**, 39–51.